Research Experience for Undergraduates
May 29 – August 3, 2007
ATLSS Laboratory – Lehigh University

Impact analysis of a Self-Centering Steel Concentrically-Braced Frame.

Eddie M. Guerra (Undergraduate student, University of Puerto Rico at Mayaguez)
David Roke (Graduate Research assistant, Lehigh University)
James M. Ricles (Professor of Structural Engineering, Lehigh University)
Richard Sause (Professor of Structural Engineering, Lehigh University)

Abstract

Self-centered concentrically-braced frames (SC-CBF) are being developed to permit large drift levels without damaging the frame members by permitting the frame to rock at its base. The rocking behavior is a rigid body motion that develops at the base of the frame, allowing one column of the frame to decompress and uplift. When the frame returns to its original position, the uplifted column impacts against the substructure. To determine the magnitude of this impact, where damage will occur and the response of the basement connections, a steel braced connection specimen was subjected to testing. This research will demonstrate how a steel braced connection located in the substructure of an SC-CBF reacts against the impact of a frame column carrying half the weight of the structure.

Introduction

Recent researches have demonstrated that SC-CBF reduce lateral drift and post-earthquake damages of a structure. The mechanism of this type of frame is based on providing the structure a rocking behavior at the base in order to self-center after the lateral loads dissipates in one direction. When the SC-CBF self-centers, the uplifted column impacts the substructure connection. This impact can generate a huge momentum at the substructure connections. Fig. 1 and Fig. 2 illustrate how the SC-CBF behaves against lateral loads and where the impact will occur.

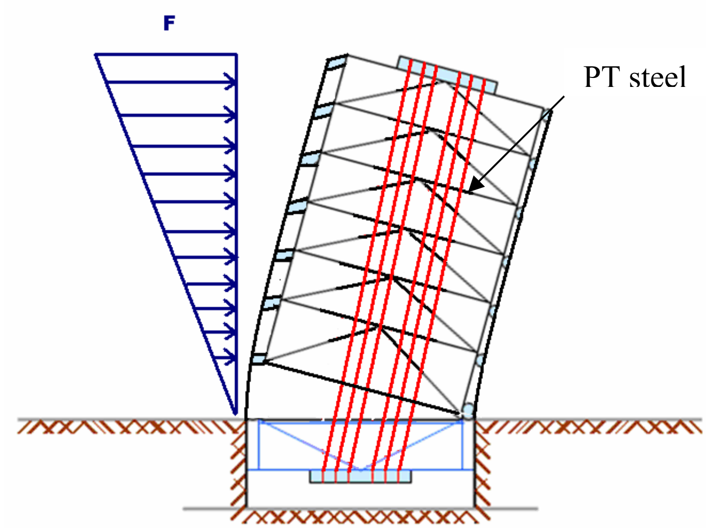

Figure 1: SC-CBF under lateral seismic loading.

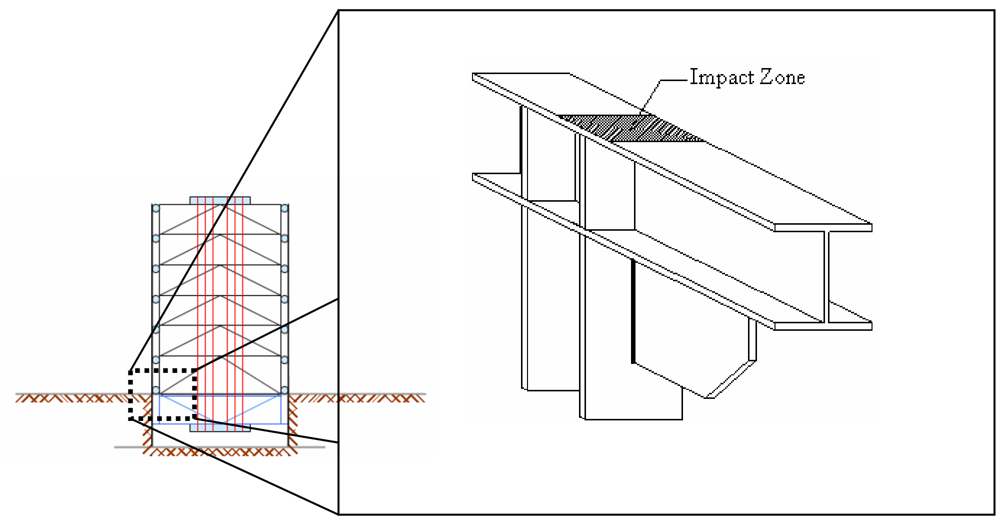

Figure 2: Impact area after column uplift

It is well known that a well design steel connection has the ability to transfer a huge amount of force through all its members. But when the connection is undergoing non-cohesive impacts the analysis becomes more difficult. Focused research on the impact between the substructure connection and the SC-CBF's uplifted column is needed.

First, it is necessary to explain how and when the SC-CBF produces the contact with the substructure. After providing a good detailed background on this mechanism, the procedure for test results will be explained. The procedure first shows how the loads acting on the base frame were determined. After this analysis, the connection is design. After the design of the entire connection, the connection is fabricated. Finally the explanation of the test setup is given.

The connection design was based on the load capacity of the SC-CBF, but in this test forces of those magnitudes will not be applied to the specimen; instead the only forces in the connection will be generated by the impact of the frame column. The projects principal focus is how the connection specimen will react against the impact load applied by the drop hammer and the extent of the damage to the connection.

Global System Behavior Background

In order to have a better understanding of the main purpose of the project, a well detailed explanation of the dynamic response of the SC-CBFs against earthquake loads is required.

SC-CBFs are being designed for better behavior of structures under earthquake loading to reduced residual drift. The frame consists of beams, columns and braces in a conventional arrangement, with column base details that permit the tension column to uplift at the foundation. A representation of a SC-CBF system is presented in Fig. 3.

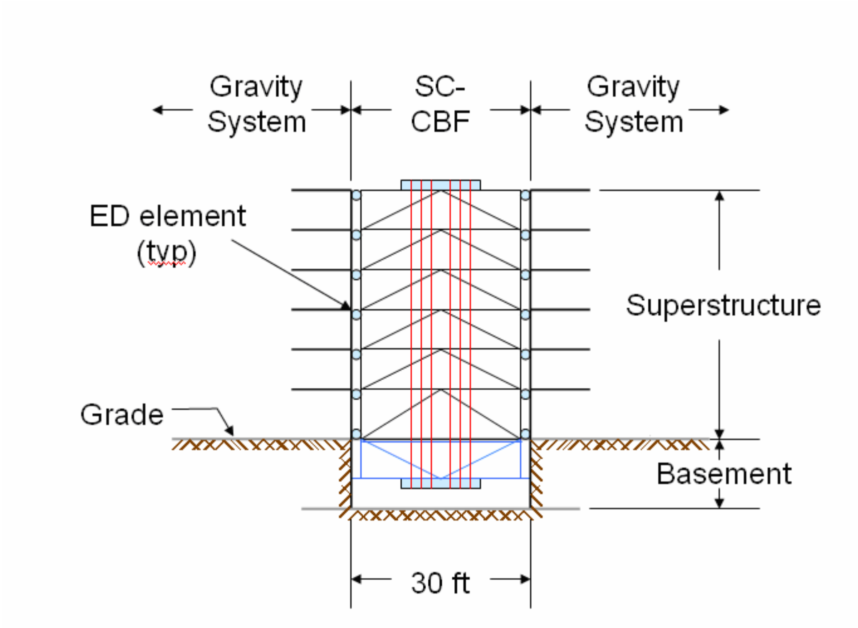

Figure 3: Self-Centering CBF.

For the design of such systems, there are a number of limit states that must be considered. These are the decompression and uplift of the tension column at the base of the frame, yielding of the post-tensioned steel, yielding of the members in the frame and buckling of the members in the frame.

Recent investigations have focused on a variety of configurations of SC-CBFs, some of them with energy dissipation (ED) elements (e.g., Sause et al. 2006). Seismic response analyses have shown that these elements have an important effect on the system response, reducing the drift of the frame and the associated column uplift under earthquake loading. For these preliminary studies, the ED element has been modeled as a simple elastic-plastic friction element.

For static analysis purposes it was assumed that the impact between the uplifted column and the base connection would act as an elastic collision; the total kinetic energy of all the particles participating in the collision is the same before and after the event. So the total energy transferred from the contact column through the substructure connection remains constant. In the final results discussion it will be explained how was the real impact registered at the substructure connection.

Design summary

The design procedure will be divided in three sections:

1. Design of the 6-story SC-CBF
    a. Capacity-based member selection
    b. Check for self-centering requirements
2. Design of the basement anchorage based on external loads and moments
    a. Determination of forces and moments acting through the frame
    b. Member selection
3. Design of connection test specimen
    a. Selecting appropriate scale
    b. Selection of members, bolts and welds

Design procedure for the 6-story SC-CBF

To start the SC-CBF design it was necessary to have an initial response of the frame against the earthquake loads; so the design process will start with an estimate of the forces in the members. An initial weight for the entire frame was assumed and then the external forces due to the earthquake were applied. The frame system under investigation is illustrated in Fig. 4(a) and 4(b).

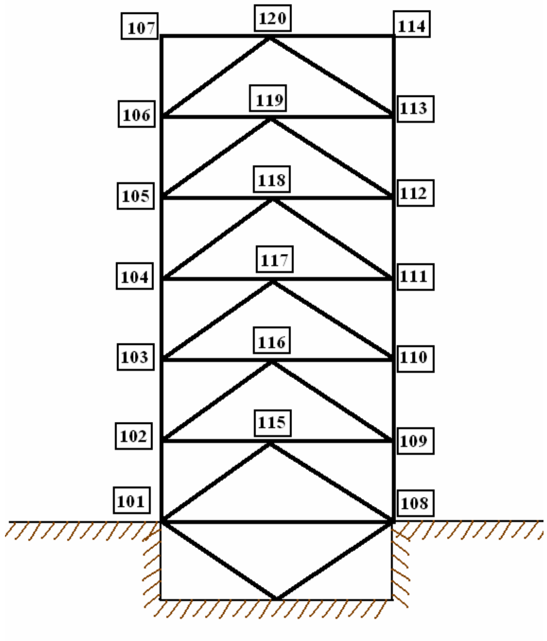

Fig. 4(a): Node numbering

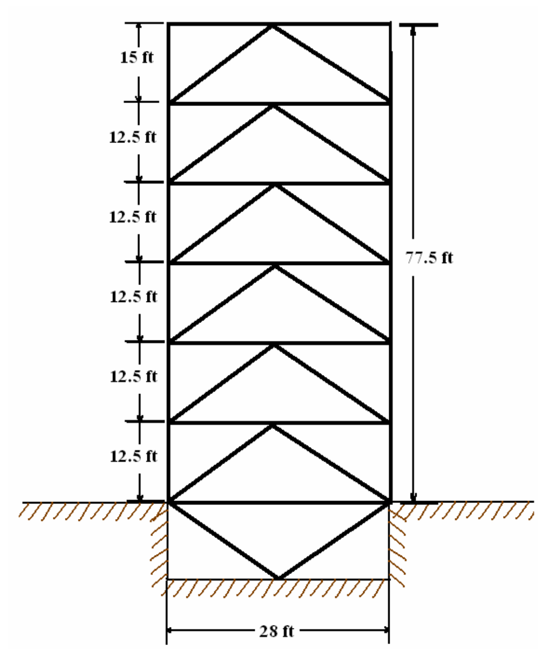

Fig. 4(b): Frame dimensions

* Note that only the lateral-load-resisting system is shown for simplicity.

As can be seen, the whole process started by numbering all the nodes of the frame. This is the full size prototype under investigation: a 6-story frame that consists of columns, beams and braces in a conventional configuration.

The dimensions and forces are already determined: everything needed to start the member selection for the SC-CBF. This is not the usual member selection procedure in a steel design. For this process the OpenSees software was used to make sure that the designed frame satisfies the criteria to behave like an SC-CBF. These criteria include the self-centering of the frame, yielding of the PT steel and non-gap opening after it self-centers. The use of OpenSees for the design process took more time than expected because sometimes the member selection satisfies the load capacities, but the frame did not behave as an SC-CBF.

To determine the design demands the moments acting in the braces were neglected, but the columns and beams were subjected to axial load and flexure. The use of formulas (H1-1a) and (H1-1b) from the Steel Construction Manual, verifies that the interaction of flexure and compression in the members were less than or equal to 1.0. Fig. 5 illustrates a simple flowchart of the interaction check.

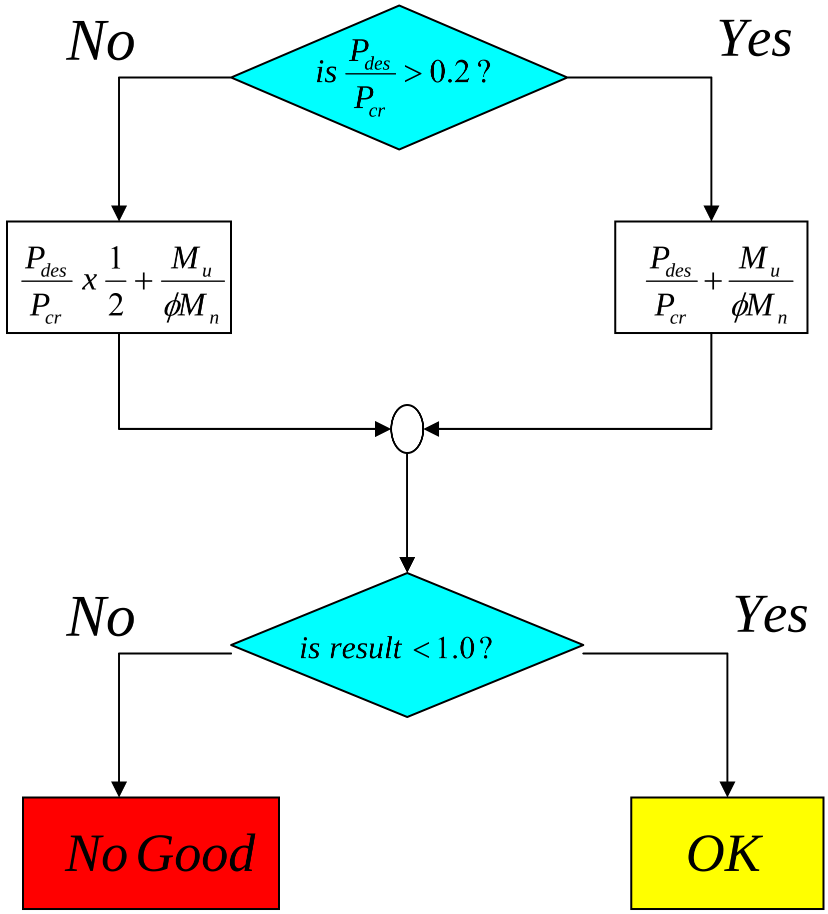

Figure 5: Interaction analogy for members under axial loads and flexure.

When all members satisfied the interaction condition, the 6-story full-scale SC-CBF design was complete. Tables 1, 2, and 3 demonstrate the final member selection as well as the other design parameters.

Braces							
Story	Design Force k	Brace Height ft	Frame Width ft	Brace Length ft	Member	Weight/ft lbs	Pcr
1	723.678	15	28	20.51828	HSS 14x10x5/8	93.1	822.4814
2	581.393	12.5	28	18.76832	HSS 12x10x1/2	69.1	632.787
3	534.766	12.5	28	18.76832	HSS 9x9x5/8	67.6	576.3069
4	440.547	12.5	28	18.76832	HSS 9x9x1/2	55.5	475.5458
5	370.123	12.5	28	18.76832	HSS 8x8x1/2	48.7	386.3563
6	2537.21	12.5	28	18.76832	W14x257	257	2737.175

Table 1: Brace properties and member selection.

Columns							
	Story	Column					
	Height	Length		Weight/ft		φMp	
Story	ft	ft	Member	lbs	Pcr	k-ft	φMn
1	15	15	W14x257	257	2960.85	1830	1826.80
2	12.5	12.5	W14x257	257	3089.20	1830	1846.78
3	12.5	12.5	W14x257	257	3089.20	1830	1846.78
4	12.5	12.5	W14x193	193	2312.08	1330	1344.02
5	12.5	12.5	W14x193	193	2312.08	1330	1344.02
6	12.5	12.5	W14x193	193	2312.08	1330	1344.02

Table 2(a): Column properties and member selection.

Compression Column				
Design	Design			
Force	Moment			
k	k-ft	Pdes/Pcr	Mu/φMn	INTERACTION
2916.38	20.10	0.98	0.01	0.99
2534.52	123.09	0.82	0.07	0.88
2188.51	78.84	0.71	0.04	0.75
1917.17	65.51	0.83	0.05	0.87
1703.97	267.86	0.74	0.20	0.91
8.04	211.72	0.00	0.16	0.16

Table 2(b): Compression column interactions check

Tension Column				
Design	Design			
Force	Moment			
k	k-ft	Pdes/Pcr	Mu/φMn	INTERACTION
497.62	70.27	0.17	0.04	0.12
860.20	252.91	0.28	0.14	0.40
1191.51	173.14	0.39	0.09	0.47
1458.13	201.30	0.63	0.15	0.76
1597.88	66.27	0.69	0.05	0.73
86.75	163.39	0.04	0.12	0.14

Table 2(c): Tension column interaction check

Beams								
	Design	Frame	Beam					
	Force	Width	Length			Weight/ft		
Floor	k	ft	ft	Member	lbs	Pcr		Pdes/Pcr
2	468.979	28	14	W27x94	94	1012.781	OK	0.463
3	422.906	28	14	W27x94	94	1012.781	OK	0.418
4	379.651	28	14	W27x94	94	1012.781	OK	0.375
5	391.719	28	14	W27x94	94	1012.781	OK	0.387
6	1884.06	28	14	W36x232	232	2489.906	OK	0.757
Roof	138.309	28	14	W27x94	94	1012.781	OK	0.137

Table 3(a): Beams member selection for axial loads

Floor	Frame Width ft	Beam Length ft	Design Moment k-ft	Member	φMp k-ft	φMn k-ft	Mu/φMn	Interaction	
2	28	14	328.54917	W27x94	1040	629.31	0.522	0.927	OK
3	28	14	345.8975	W27x94	1040	629.31	0.550	0.906	OK
4	28	14	318.19167	W27x94	1040	629.31	0.506	0.824	OK
5	28	14	249.81333	W27x94	1040	629.31	0.397	0.740	OK
6	28	14	508.60333	W36x232	3510	2561.35	0.199	0.933	OK
Roof	28	14	466.98417	W27x94	1040	629.31	0.742	0.810	OK

Table 3(b): Beam member selection for moment capacities.

Design of the basement anchorage based on external loads and moments

Based on a static analysis of the entire basement anchorage system as shown in figure 7, the forces acting at each member of the structure were determined. The first step was to analyze the forces acting directly to the substructure due to the influence of the earthquake loads, the shear forces produced by the energy dissipation elements, the tensile force of the PT steel and of course the weight of the 6-story frame. Fig. 7 shows a free body diagram of the basement anchorage.

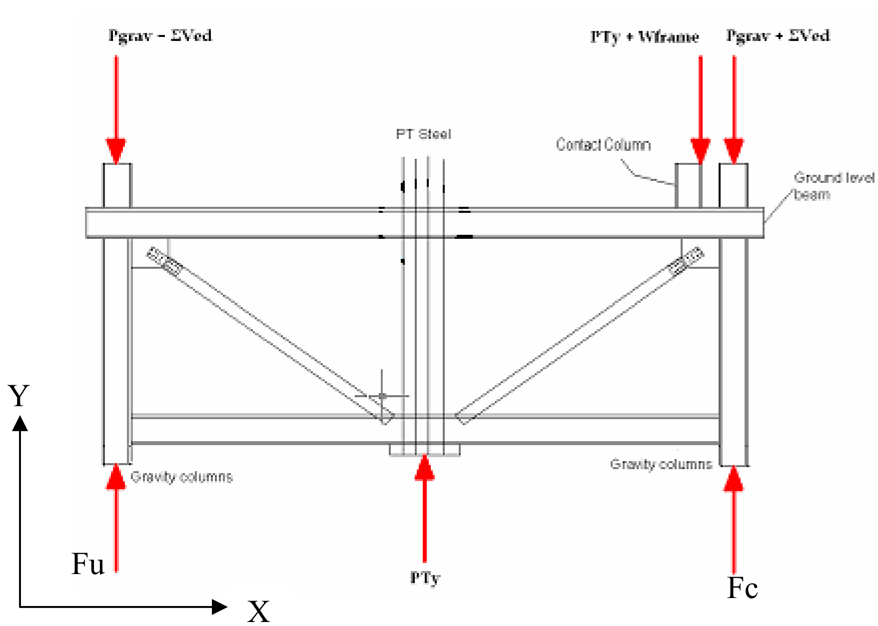

Figure 6: Basement anchorage free body diagram

All forces acting on this frame were determined by prior analyses. The P_{grav} force is equal to 972 k and represents the sum of gravity loads on one gravity column of the SC-CBF. The ΣVed is the result of the reaction of the energy dissipation elements against the vertical displacement of the SC-CBF. This force is equal to 252 k. When one of the tension gravity columns decompresses, the PT steel acting on the center of the entire frame will develop a force equal to 3413 k, this is the PTy force represented in the previous diagram. The weight of the SC-CBF (Wframe) was calculated after all the members were selected. This force is equal to 77.2 k.

Basic equilibrium equations and the computer software SAP were used to determine the force acting in each of the members. The following equations were used and the SAP software was used to verify the results:

Equation (1)

$$M_{bframe} = \alpha_y M_{ELF} - \sum V_{ED} * (b_{frame} + d_{fr}) - 2\sum V_{ED} * S - PT_y * \frac{1}{2}(b_{frame} + d_{fr}) - W_{frame} * \frac{1}{2}(b_{frame} + d_{fr})$$

Equation (2)

$$F_c = \frac{\alpha_y M_{ELF}}{b_{frame} + d_{fr}} - \sum V_{ED} * \frac{d_{fr}}{b_{frame} + d_{fr}} + \frac{1}{2} * W_{frame} + P_{grav}$$

Equation (3)

$$F_u = \frac{\alpha_y M_{ELF}}{b_{frame} + d_{fr}} - \sum V_{ED} * \frac{d_{fr}}{b_{frame} + d_{fr}} - \frac{1}{2} * W_{frame} - P_{grav}$$

Where: α_y = 1.4 = ratio of base overturning moment required to yield PT bars to M_{ELF}

M_{ELF} = 37551 k-ft, overturning moment caused by lateral forces.

b_{frame} = centerline to centerline spacing of frame columns = 26.33 ft

d_{fc} = depth of frame column = 16.4 in

The next step was to verify the values obtained from the equilibrium equations using SAP2000©. From Eq. (1) the overturning moment acting on the frame was determined to be about 3680 k-ft. The results from Eq. (2) and (3) shows the reactions at the foundation. The force acting below the uplifted column and below the contact column were 874 k and 2896 k, respectively. These two forces, Fu and Fc, were equal to the forces determined by SAP2000©. Fig. 8 shows the substructure model and the applied loads. Table 4 shows values of the axial forces determined by SAP2000.

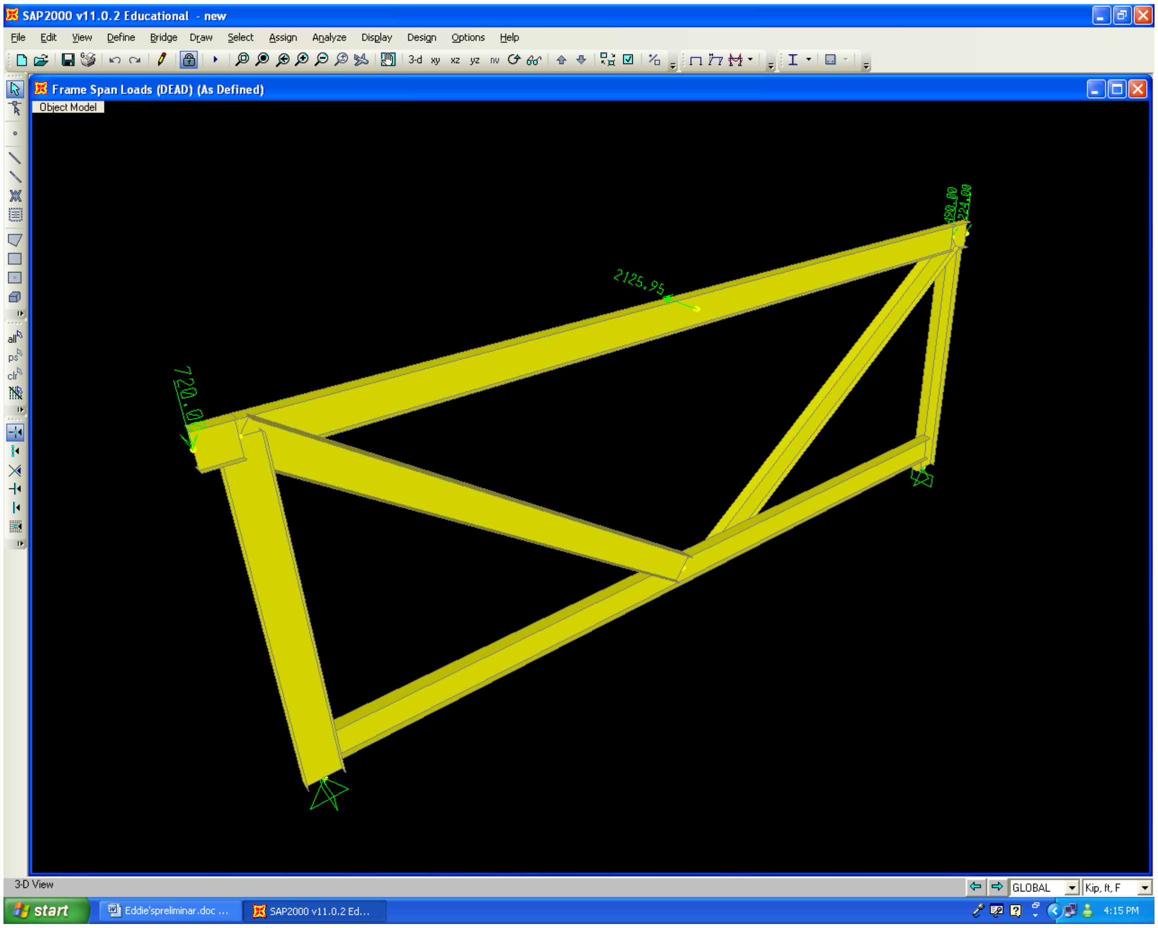

Figure 7: Basement anchorage model

Frame	Station	OutputCase	CaseType	P
Text	ft	Text	Text	Kip
1	0	DEAD	LinStatic	874.649
2	1	DEAD	LinStatic	-2977.194
3	27.706	DEAD	LinStatic	2463.128
4	0	DEAD	LinStatic	192.525
5	16.1072	DEAD	LinStatic	-2970.003
6	0	DEAD	LinStatic	-2777.101

Table 4: Axial forces acting in substructure members.

Member selection for 1/3 scaled connection

Before selecting the column, beam and brace that will be required for the connection, the scale factors for the forces, lengths and moments were determined. It was decided to reduce the full-scale model to a 1/3-scale model because of the limited space that was available at the drop-hammer test machine. The lengths of the members were reduced to 1/3 of the full size, the forces were reduced to 1/9 of the original magnitude and the moments were scaled by 1/27.

To make a less complicated fabrication process, identical sections were selected for the beam, column and brace. By selecting a W8 x 40, all load capacities were satisfied. The braces were subjected to compression, but since the moments and shears acting in the brace were so small, they were neglected. In that way the brace was analyzed as a column under pure axial loading. In Table 4-1 of the AISC manual it can be seen that a W8 x 40 member of 5.4 ft subjected to compression can hold a force of 309 k. Also in the same table, it can be seen that the column section will satisfy the required axial force of 322 k. It was checked that it will also satisfy the flexure capacity in Table 3-2. For the beam capacity it can be seen in Table 5-1(Available strength in axial tension) and in Table 3-2(Flexural design) and the selection is appropriate for both load conditions.

To speed up the fabrication process, it was a good idea to use W8 x 35 beams available at the ATLSS facilities. So it was necessary to first determinate if it was feasible to use this section size. It was assumed that the specimen will never experience such loads and moments during the test procedure. Finally, it was decided to use the W8 x 35 sections for the beam, brace and column in the connection. It is important to mention that the same interaction criteria that were used for the member selection of the SC-CBF frame established by the AISC Steel Construction Manual, were also used for the design of the 1/3-scale connection specimen. In Tables 2(a), 2(b), 2(c), 2(d) & 2(e) is demonstrated the design parameters as well as the member selection.

Braces						
Design Force k	Brace Height ft	Frame Width ft	Brace Length ft	Member	Weight/ft lbs	Pcr
330	3.08	4.39	5.37	W 8x40	40	452.65

Table 5(a): Brace member selection

Foundation Columns						
Story Height ft	Column Length ft	Member	Weight/ft lbs	Pcr	φMp k-ft	φMn k-ft
3.42	3.42	W8x40	40	511.03	149	158.37

Table 5(b): Column member selection

Foundation Contact Column				
Design	Design			
Force	Moment			
k	k-ft	Pdes/Pcr	Mu/φMn	INTERACTION
321.76	45.73	0.63	0.29	0.89

Table 5(c) : Axial force and moment interaction for column

Beams								
Design	Design	Frame	Beam					
Force	Moment	Width	Length		Weight/ft	Pcr	φMn	Mu/φMn
k	k-ft	ft	ft	Member	lbs	k	k-ft	k-ft
273.68	74.99	10	10	W8x40	40	427.78	117.09	0.64

Table 5(d): Beam member selection

Bolts, welds and plates selection

The next and final step for the design of our connection specimen was the selection of the bolt nominal diameter, the size of the fillet weld, and the thickness of the plates in the connection. Fig. 9 illustrates the final connection design.

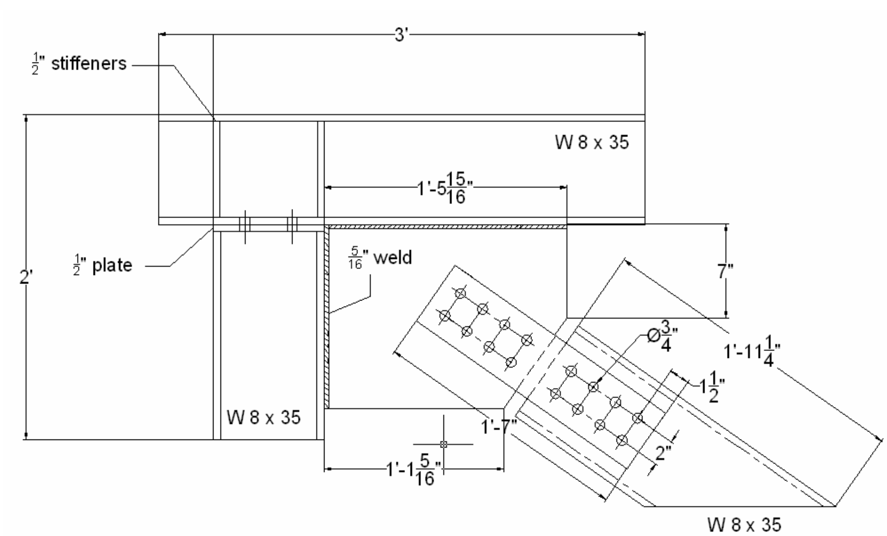

Figure 8: Sketch of the 1/3 connection specimen

The bolt diameter selection was determined so that it satisfies the axial load coming from the brace. From Table 7-1 of the AISC steel construction manual, the bolts selected were ¾” diameter, A490-X bolts. The bolts will be in double shear because in this way a fewer bolts are required to resist the shear force in the connection. Also the connection length will be smaller. The weld used to connect the gusset plate to the column and beam was a 5/16”fillet weld. The smallest weld size was selected and checked if it will resist the horizontal and vertical components of the axial force coming through. Fig.10 shows the connection details.

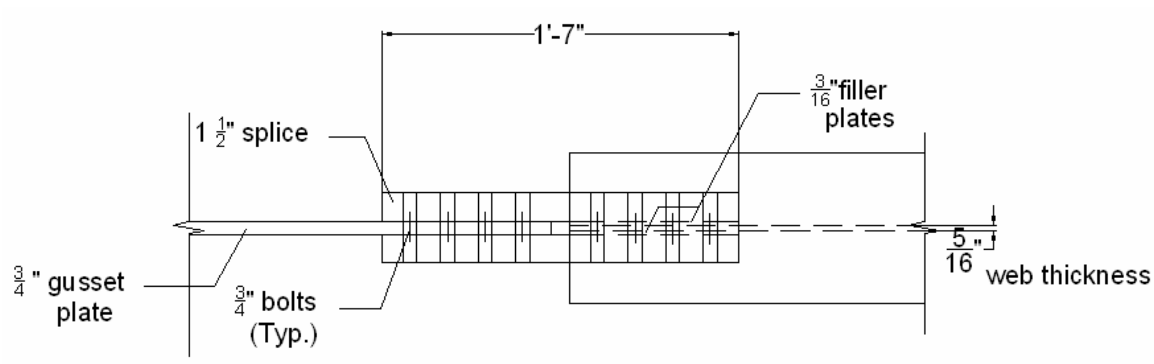

Figure 9: Connection details.

The use of two splice plates of 1.5” thickness was required. The thickness of the splice plates was based on the limit states of yielding, tensile rupture, and block shear rupture. The size of the gusset plate was also determined by these criteria. After selecting the thicknesses of these elements, the W8 x 35 beams were also checked for these limit states.

Fabrication Process

All the drawings for the connection and members details were made using AutoCAD2005. In a period of 4 to 5 days the connection specimen was done and ready to be tested. Picture 1 shows the area where the specimen was fabricated.

Figure 10: Specimen fabrication.

Test setup

At almost the same time that the specimen was under construction, the test setup at Fritz Laboratory facilities was being planned. The following is a summary of the steps that were followed for making this a successful test:

1. Meeting with Lab technicians for scheduling of test process
2. Hand in test program and work order to lab technicians
3. Hand in drawings of specimen and placement details to technicians
4. Verification of final settlement of the specimen in the test machine
5. Hand in test parameters. This includes weights and heights needed for the drop weight
6. Preparation for the settlement of video camera devices and lights
7. Perform test
8.

The following pictures illustrate how the experimental site was developed.

Figure 11: Connection Specimen in drop hammer machine.

Figure 12: Connection Specimen

Figure 13: Connection Specimen

Figure 14: Lights and camera settings.

Figure 15: High Resolution Camera

Determination of test parameters

In order to proceed with the drop weight test, the values of two very important parameters were required: the different heights that the drop hammer will be dropped and the weight that the drop hammer will carry. Scaling factors had to be applied to the weight of the whole structure and the velocity with which the frame is moving during its rocking behavior. The total weight was determined after the selection of the members and it was found that it is 77.2 kips. Velocity values were obtained as a result of dynamic analyses performed by OpenSees. First the whole frame was divided into tributary areas, around each column node of the SC-CBF, and then the quantity of mass carried at each node was calculated. There were made 5 different dynamic analyses with OpenSees, the first one with vertical masses at the nodes, then double of the vertical masses at the nodes, half of the vertical masses at the nodes, 3/2 of the vertical masses at the nodes and finally with all of the vertical masses concentrated at nodes 102 and 109. The maximum velocity obtained from all the different analyses was about 18.005 inches/sec. Finally a velocity of 20 inches/sec. was assumed as a conservative value to use as the velocity of the full scale model.

A constant weight of 486 pounds for the drop hammer was established. This weight also includes the column stub attached to the drop hammer. This was the weight that was dropped from different heights. The following equations summarize the procedure for selecting and relating the weights, velocities and momentums generated by the test with the full-scale size model.

Total mass of full scale model = mf = $\left(\frac{1}{2 \cdot g}\right) \cdot \text{Wframe} =$ mf = $\left(\frac{1}{2 \cdot 386.4}\right) \cdot 77.2 = 0.1 \quad k \cdot \frac{s^2}{in}$

Total mass of 1/3 scale model = $m_{(1/3)}$ = $\lambda^2 \cdot mf = (0.33333)^2 \cdot 0.1 = 0.011 \quad k \cdot \frac{s^2}{in}$

Velocity full scale full weight = vf = 20 in/sec.

Velocity 1/3 scale full weight = $v_{(1/3)}$= $\sqrt{\lambda} \cdot vf = \sqrt{\lambda} \cdot 20 = 11.547 \quad \frac{in}{sec}$

Total momentum of 1/3 scale model = $m_{(1/3)} * v_{(1/3)}$ = $0.011 \cdot 11.547 = 0.127 \quad k \cdot sec$

Table 3 demonstrates the variable heights from which the weight was dropped. Also it shows the relations between the weight of the drop hammer and the weight of half of the full-scale frame ($Ws/W_{frame/2}$). The relation between the momentum generated by the scale model and the one generated by the full-size model is also an important factor to study.

			Variable height		sqrt(2*H*g)	mass*Veloc.	Momentum/ Total momentum of scaled model
Total weight to be dropped (k)	mass (k-s^2/in)	$W_s/W_{frame/2}$ (%)	Height (in)	Height (ft)	Velocity (in/sec.)	Momentum	M_s/M_{frame} (%)
0.486	0.00126	11.45	3	0.25	48.150	0.061	47.3
0.486	0.00126	11.45	6	0.5	68.094	0.086	66.9
0.486	0.00126	11.45	12	1	96.300	0.121	94.6
0.486	0.00126	11.45	15	1.25	107.666	0.136	105.8
0.486	0.00126	11.45	21	1.75	127.392	0.160	125.1
0.486	0.00126	11.45	30	2.5	152.263	0.192	149.6
0.486	0.00126	11.45	60	5	215.332	0.271	211.5
0.486	0.00126	11.45	120	10	304.526	0.383	299.2

Table 6: Test parameters and the relations between scaled and full size model.

Test procedure

As shown in the previous table, a total of 8 drops with variable heights were performed. Before each drop, the use of safety hardware like hard hats and ear protection was required for all attendees. The weight used for each drops was 486 pounds, which represents almost 11.5 % of half of the total weight of the 1/3-scaled SC-CBF. The procedure was simple: (1) first the lab technician measured the height from which the column drop hammer was going to be dropped. This height is measured from the bottom of the column stub to the surface of the top flange of the specimen. (2) When the video was ready to record, the weight was dropped against the specimen. (3) Finally, immediately after the impact, observations of the entire connection were made, looking for indentation deformations, cracks in welds, and an overall review of the connection. The following pictures illustrate the testing procedure.

Figure 17: Lab technician taking measurements before drop.

Figure 18: Specimen ready for impact test.

Test results and analysis

Damages on the connection were not significant after the entire testing regimen. This may seem to suggest that the connection performed perfectly against these impacts, but there are very important and detailed observations that needs to be considered. The focus of this analysis will be two aspects: deformation and collision behavior.

The only area on the specimen that suffered visible damage was the top flange of the horizontal beam. The indentation in that area was caused by the repeated impacts against the specimen. These small changes in the surface of the top flange were measured with feeler gages specially used for small indentation deformations. The measurements were done along a centerline on top of the beam web. Fig. 11 shows the damage zone of the top flange and the measured reduction in the flange thickness.

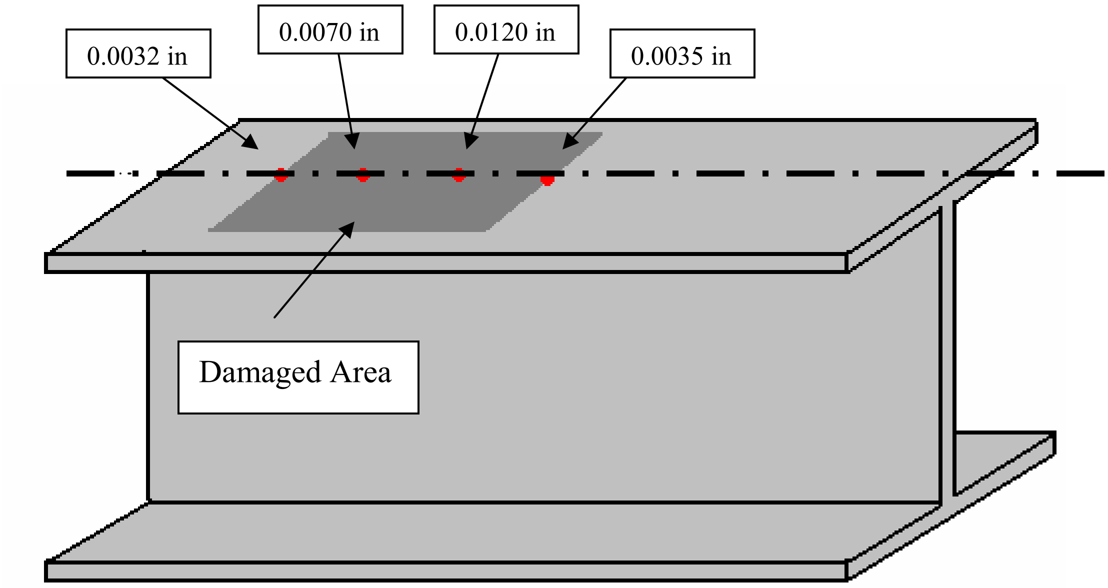

Figure 19: Sketch of specimen showing damage area and measured points.

Note that the entire specimen did not experience significant damages during the testing process. Even at the end of the testing, been subjected to impacts greater than they are supposed to be in the full-scale model, resultant damages were no taken as significant.

The welded section between the column stub and the ½" base plate was another point of interest that was examined after the impact test. There were expectations that the welds will develop some cracks at the toe or root of the welds, so the base of the column stub was cut about 3" from the base. A total of 7 cuts were made as shown in picture 9. Picture 10 shows how a x20 microscope was used to look for any cracks in the welds. No cracks were found in any of the welds.

Figure 20: Sliced bottom part of the column stub

Figure 21: Visualizing welded sections

During the test it was observed that the collision between the drop weight and the specimen behave as a totally non-cohesive impact and the maximum rebound heights developed were higher than expected. Table 4 shows how many times the 486 pounds drop weight rebounded and the maximum height achieved after the first rebound. These values were determined with the help of the high quality videos taken during testing.

Test #	Maximum height (in)	# of rebounds
1	1.0	4
2	1.5	4
3	3.0	4
4	4.5	4
5	6.0	4
6	7.5	4
7	16.0	5
8	25.5	6

Table 7: Maximum heights and number of rebounds for each test.

(a) (b)

Figure 22(a) & 22(b): Final views of impact zone after testing.

Acknowledgments

The work described in this paper would not be possible without the support of the National Science Foundation (NSF) and the Network for Earthquake Engineering Simulation program (NEES). Also I want to give special thanks to my mentor David Roke and faculty advisors, Dr. James Ricles and Dr. Richard Sause. Technical and lab procedures could not be done without the great help of Peter Bryan, Gene Matlock, John Hoffner and Carl Siegrist.

References

American Institute of Steel Construction (AISC), (2005). *Manual of Steel Construction – LRFD*, 13rd Edition.

R. Sause, J. M. Ricles, D. Roke, C.-Y. Seo, and K.-S. Lee, (2006). *"Design of Self-Centering Steel Concentrically-Braced Frames"* 4th International Conference on Earthquake Engineering.

SAP 2000 Educational 11.0.2, Structural Analysis Program, Copyright 1976-2005 Computers & Structures Inc.

OpenSees – Open System for Earthquake Engineering Simulation, Pacific Earthquake Engineering Research Center – version 1.7.0, Copyright 1999 the Regents of the University of California.